Negative-parity states of Er isotopes in the interacting-boson-plus-a-fermion-pair model

S. T. Hsieh
Department of Physics, National Tsing Hua University, Hsinchu, Taiwan, Republic of China

D. S. Chuu
Department of Electrophysics, National Chiao Tung University, Hsinchu, Taiwan, Republic of China
(Received 26 July 1990)

The energy levels of negative-parity states of even-even isotopes ^{156}Er, ^{158}Er, and ^{164}Er are studied in terms of the interacting s-, d-, and f-boson-approximation model and allowing one s or d boson to break and form a fermion pair. In the calculation two single fermion orbits $h_{11/2}$ and $i_{13/2}$ are considered. The energy levels of the negative-parity bands of these nuclei can be reproduced satisfactorily.

I. INTRODUCTION

Recent experimental studies of the level energies for both even- and odd-mass nuclei in the erbium region have provided an abundance of data.[1–13] Among these data, the anomalous negative-parity bands have been observed and the phenomenon of backbending occurs as one plots the moment of inertia versus the square of the angular velocity for yrast band of a nucleus. The backbending of the moment inertia at high spin is generally believed to be a result of the complicated interplays between the collective and the single-particle degrees of freedom induced by the Coriolis decoupling.[14] A generalized calculation within the framework of the two-quasiparticle plus rotor bandmixing model[15] predicted that the high-spin states are produced by the alignments of the angular momenta of the decoupled quasiparticles along the collective rotation, and the observed backbends are attributed to the intersection of the zero-quasiparticle band and the decoupled two-quasiparticle band.

The interacting-boson-approximation (IBA) model[16] and its extension[17] have been successful in the description of the collective states in many media to heavy even-even nuclei. Recently, some high-spin negative-parity bands of Er isotopes had been identified by in-beam studies.[1–3,7,8,18] It is hopeful to expect that the properties of these negative-parity bands can also be interpreted by the extended IBA model.

In this work, we shall study the structures of the negative-parity bands of even-even ^{156}Er, ^{158}Er, and ^{164}Er isotopes. These nuclei are all well known for the structure change at high spin, and their abundant negative-parity bands provide a good testing example of the extended IBA model. The IBA model with one f or one p boson included in the calculation has been applied to study the negative states of $N=88$ isotones.[19] It was found that the states below $I\simeq 17$ could be reproduced quite well. In order to interpret the higher-spin states which were observed more recently , one can incorporate the traditional IBA model with one f boson (sdf IBA) and allow an s or d boson to have the fermion-pair degree of freedom. To make the calculation feasible, we include only one f boson and consider only two single-particle orbits. In the region of well-deformed nuclei the unique parity intruder orbitals such as $h_{11/2}$ and $i_{13/2}$ are generally believed to be the most important because both the Coriolis antipairing effect and the rotation alignment effect increase with increasing angular momentum.[20] Therefore, we include only these two single-particle orbits in the present calculation. Furthermore, the IBA-1 basis states are used in the boson core in this work. It was shown that the difference between IBA-1 and IBA-2 was less prominent in the transitional regions far from the closed shell.[21]

II. MODEL

In the calculation of the energy levels of Er isotopes, $Z=N=82$ is taken as the core, pure IBA assumes a valence s- and d-boson number $N_B=9$, 10, and 13 plus an f boson for the three nuclides, ^{156}Er, ^{158}Er, and ^{164}Er, respectively. In addition to the pure boson configuration, we admix the N_B-1 sd boson and one f boson plus one fermion-pair configuration into the model space:

$$|n_s n_d v\alpha L, f; L_T M_T\rangle \oplus |[n_s' n_d' v'\alpha' L', j^2(J)]L_c, f; L_T M_T\rangle ,$$

where $n_s+n_d=N_B$, $n_s'+n_d'=N_B-1$, $j=\frac{11}{2}$ or $\frac{13}{2}$, and $J\geq 4$. The total boson number is $N=N_B+1$. The $J=0$ and 2 fermion-pair states are excluded to avoid double counting of the states. The model Hamiltonian consists of four parts:

$$H=H_B+H_F+V_{BF}+V_N ,$$

where H_B is the IBA boson Hamiltonian,

$$H_B=a_0 n_d+a_1 P^\dagger\cdot P+a_2 L\cdot L+a_3 Q\cdot Q .$$

The fermion Hamiltonian H_F is

$$H_F=\sum_{j,m}\varepsilon_j a_{jm}^\dagger a_{jm}+\tfrac{1}{2}\sum_{j,J}V^J(a_j^\dagger a_j^\dagger)^J\cdot(\tilde{a}_j\tilde{a}_j)^J ,$$

where ε_j is the fermion single-particle energy, V^J's are the fermion-fermion interactions, and $a_j^\dagger$ ($\tilde{a}_j$) is the nucleon creation (annihilation) operator. The mixing Hamiltonian V_{BF} is assumed:

$$V_{BF}=\alpha Q^{B}\cdot\sum_{j}(a_j^{\dagger}\tilde{a}_j)^{(2)}+\beta Q^{B}\cdot\sum_{j}[(a_j^{\dagger}a_j^{\dagger})^{(4)}\tilde{d}-d^{\dagger}(\tilde{a}_j\tilde{a}_j)^{(4)}]^{(2)},$$

where

$$Q^{B}=(d^{\dagger}\tilde{s}+s^{\dagger}\tilde{d})^{(2)}-(\sqrt{7}/2)(d^{\dagger}\tilde{d})^{(2)},$$

and the Hamiltonian related to the f-boson part is

$$V_N=\varepsilon_f n_f+\gamma Q^{B}\cdot(f^{\dagger}\tilde{f})^{(2)}+\delta\sum_{j}(a_j^{\dagger}\tilde{a}_j)^{(2)}\cdot(f^{\dagger}\tilde{f})^{(2)}.$$

To keep the number of interaction parameters to be minimum, we assumed that the mixing parameters α, β, γ, and δ do not have microscopic structure (i.e., they do not depend on j). Furthermore, the α, β, γ, and δ are assumed to be constants for the three isotopes. This is because in the IBA calculation, the interaction parameters in general vary with different isotopes, while in the shell-model calculation the interaction parameters can be unified for a certain mass region.[22,23] Since the variation with the boson number of the interaction parameters α, β, γ, and δ in the mixing Hamiltonian for bosons and fermions can be absorbed by the boson interaction parameters a_0, a_1, a_2, and a_3, therefore, it is reasonable to assume that the interaction parameters α, β, γ, and δ are constants for different isotopes.

In the calculation, the radial dependence of the fermion potential is taken as the Yukawa type with a Rosenfeld mixture. An oscillation constant $\nu=0.96A^{-1/3}$ fm^{-2} with $A=160$ is assumed. The strengths of V^{J}'s are determined by requiring $\langle jj|V|jj\rangle_{j=2}-\langle jj|V|jj\rangle_{j=0}=2$ MeV for $j=\frac{13}{2}$. The whole Hamiltonian is then diagonalized in the selected model space. The parameters contained in the Hamiltonian H were chosen to reproduce the negative-parity energy spectra of $^{154-164}$Er isotopes, respectively. The ε_f is set to be zero because all the states considered in our calculation contain one f boson. The interaction strengths and the single-particle energies for each isotope are allowed to be mass-number dependent.

III. RESULTS

Table I presents the final searched values of the interaction strengths and single-particle energies. The mixing parameters α, β, γ, and δ are generally very small and can be unified as (in MeV) $\alpha=0.21$, $\beta=0.025$, $\gamma=-0.015$, and $\delta=0.15$. The smallness of the mixing parameters manifests the fact that the mixings between the pure boson configuration and the configuration with one fermion pair are small. From Table I one can note that the strength of the d-boson energy a_0 decreases and the strength of a_3 also decreases as boson number increases. This corresponds to the fact that the isotopes become more collective as the boson number increases. This is consistent with the tendency of deviating away from U(5) symmetry to become the SU(3) symmetry. The single-particle energies $\varepsilon(h_{11/2})$ and $\varepsilon(i_{13/2})$ are obtained as a result of fitting. In the calculation, we found if we increase the $h_{11/2}$ single-particle orbit in energy so that it becomes effectively irrelevant, then the agreements between the calculated and the observed levels with $I=19$–26 will become worse as the calculated levels with $I=27$–31 are still required to agree better with the observed values. This shows the statistical significance of the single-particle energies. From Table I one can note that the single-particle energy for $i_{13/2}$ orbit increases linearly while that for $h_{11/2}$ decreases as boson number increases. The highest observed angular momentum level $I=24$ for the nuclei ^{164}Er is dominated by the configuration of $N-1$ boson plus two $h_{11/2}$ fermions; the value of the single-particle energy $i_{13/2}$ for the nuclei ^{164}Er is obtained as a result of smoothly extrapolating. The magnitudes of pairing term $P^{\dagger}\cdot P$ and $L\cdot L$ term are somewhat correlative with the magnitudes of quadrupole term $Q\cdot Q$ and d-boson energy a_0, respectively.

The calculated and observed negative-parity energy spectra for ^{156}Er is shown in Fig. 1. From Fig. 1, one can note that the calculated results for the four negative-parity odd and even bands agree quite well with the observed data. Evidence for structure change in ^{156}Er is found in the intense feeding among four negative-parity bands. Table II lists the relative wave-function intensities for energy levels of ^{156}Er. From Table II one can note that the dominant configuration for states with $I\leq 19$ of the yrast negative-parity odd spin band are the pure boson configuration while the states with higher angular momentum are dominated by $N-1$ boson plus two $h_{11/2}$ fermions (two-proton states) or $N-1$ boson plus two $i_{13/2}$ fermions (two-neutron states) excitation configurations. For the third odd spin band, the $N-1$ boson plus one fermion-pair configuration is dominated from the state with $I=21$ up. The configuration of the $N-1$ boson plus one fermion pair in the negative-parity even band is dominated only in the state with $I\geq 22$. The importance of the configuration with $N-1$ boson plus

TABLE I. The interaction parameters in MeV for IBA-plus-one-fermion-pair model adopted in this work.

Nuclei	N_B	Parameter (MeV) a_0	a_1	a_2	a_3	$\varepsilon_{11/2}$	$\varepsilon_{13/2}$
^{156}Er	9	0.1236	−0.053	0.0075	0.0017	1.7681	1.7789
^{158}Er	10	0.1136	−0.053	0.0065	−0.0069	1.7665	1.8461
^{164}Er	13	0.0697	−0.053	0.0065	−0.0087	1.4547	1.8500

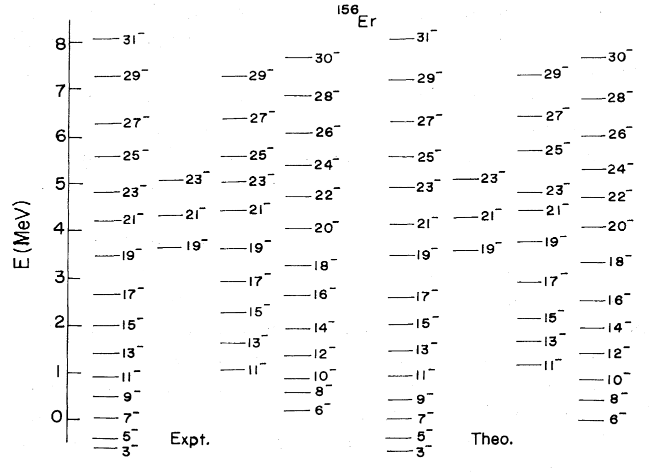

FIG. 1. The calculated and observed negative-parity energy spectra for ^{156}Er. The observed data are taken from Refs. 2 and 12.

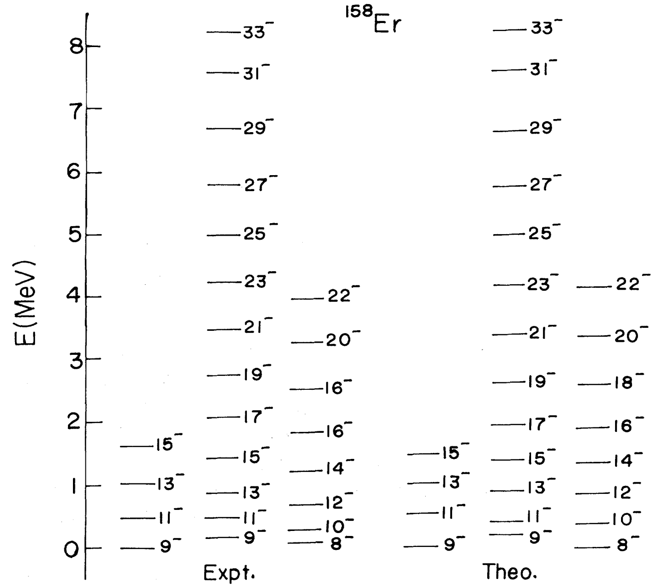

FIG. 2. The calculated and observed negative-parity energy spectra for ^{158}Er. The observed data are taken from Refs. 3, 4, and 13.

two $i_{13/2}$ fermions is exhibited only in the states with $I \geq 27$ in the yrast odd spin band, $I \geq 25$ in the third odd spin band, and $I \geq 26$ in the even spin band. The mixing between two configurations is in general very small except for the states 25_2^- (73% to 27%), 26_1^- (83% to 17%), 27_1^- (79% to 21%), 27_2^- (25% to 75%), and 28_1^- (20% to 80%). The calculated and observed energy spectra for ^{158}Er are shown in Fig. 2. There are abundant experimental data[3,4,13] observed in recent years. The negative-parity states of ^{158}Er up to 41^- were assigned definitely.[3] It can be seen from Fig. 2 that the energy levels of ^{158}Er can be reproduced satisfactorily. The analysis of the wave functions shows that the pure boson configuration is dominant in the states with $I \leq 23$ while the state 25_1^- is dominated by the configuration of $N-1$ boson plus two $h_{11/2}$ fermions. The states 31_1^- and 33_1^- are dominated by the configuration of $N-1$ boson plus two $i_{13/2}$ fermions. The mixing of these two configurations is im-

TABLE II. The relative intensities of wave functions for energy levels of nuclei ^{156}Er.

States	0	$h_{11/2}$	$i_{13/2}$	States	0	$h_{11/2}$	$i_{13/2}$
3	0.999	0.001	0.000	25	0.000	0.992	0.008
5	0.999	0.001	0.000	26	0.000	0.832	0.168
6	0.997	0.003	0.000	27	0.000	0.785	0.215
7	0.997	0.003	0.000	28	0.000	0.199	0.801
8	0.993	0.007	0.000	29	0.000	0.000	1.000
9	0.993	0.006	0.000	30	0.000	0.000	1.000
10	0.990	0.010	0.000	31	0.000	0.000	1.000
11	0.990	0.010	0.000	11_2	0.994	0.006	0.000
12	1.000	0.000	0.000	13_2	1.000	0.000	0.000
13	1.000	0.000	0.000	15_2	1.000	0.000	0.000
14	1.000	0.000	0.000	17_2	1.000	0.000	0.000
15	1.000	0.000	0.000	19_2	0.999	0.001	0.000
16	1.000	0.000	0.000	19_3	0.000	0.999	0.001
17	1.000	0.000	0.000	21_2	0.000	0.999	0.001
18	1.000	0.000	0.000	21_3	0.000	0.998	0.002
19	1.000	0.000	0.000	23_2	0.000	0.999	0.001
20	1.000	0.000	0.000	23_3	0.000	0.995	0.005
21	1.000	0.000	0.000	25_2	0.000	0.726	0.274
22	0.000	0.999	0.001	27_2	0.000	0.254	0.746
23	0.000	0.999	0.001	29_2	0.000	0.000	1.000
24	0.000	0.998	0.002				

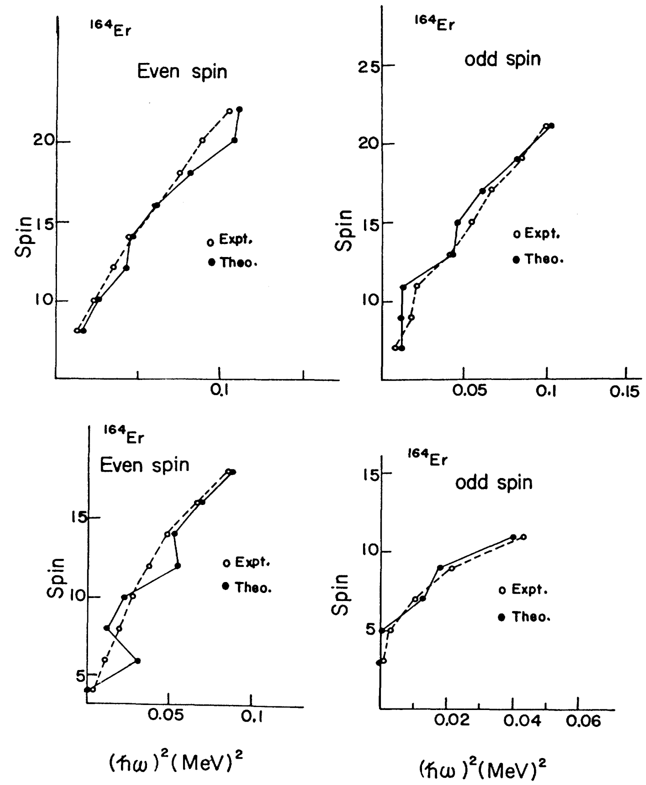

FIG. 3. The calculated and observed spin angular momentum I vs $(\hbar\omega)^2$ for negative-parity even and odd spin states of ^{164}Er.

portant only in the two states 27_1^- (79% to 21%) and 29_1^- (49% to 51%). Several possible negative-parity even and odd spin bands of ^{154}Er and ^{164}Er were observed[1,8,9,13] in the past few years. We do not present the calculated energy levels of these two nuclei here. However, the observed energy levels of these two nuclei can also be reproduced quite reasonably.

The backbends occurring in the deformed nuclei region are commonly interpreted as the transition from the ground-state rotational band to the aligned two-quasiparticle $i_{13/2}$ nucleon band.[24] Here we choose the sensitive expression as to plot the spin angular momentum I vs conventional $(\hbar\omega)^2$ curves, with

$$(\hbar\omega)^2=\left[\frac{E_I-E_{I-2}}{[I(I+1)]^{1/2}-[(I-2)(I-1)]^{1/2}}\right]^2 .$$

The plots for spin angular momenta vs $(\hbar\omega)^2$ of the negative-parity bands for ^{164}Er are presented in Fig. 3. This nuclide is in the strongly deformed region because its first excitation energy is less than 0.1 MeV. It is quite close to SU(3) due to its high-lying β and γ bands and low $\beta\rightarrow\gamma$ and $g\rightarrow\gamma$ $B(E2)$ values. Our calculation shows that the main feature of the I vs $(\hbar\omega)^2$ curve for the nuclide ^{164}Er can be reproduced reasonably well except for some fine variations. In order to explain the detailed variations existing at the higher spins, some additional mechanism such as more single-particle orbits or more fermion pairs should be considered.

IV. CONCLUSION

In summary, we have investigated the structure of the negative-parity energy spectra of the isotopes ^{156}Er, ^{158}Er, and ^{164}Er. We extend the IBA model to include an f boson to substitute for an sd boson and allow an sd boson to break into a fermion pair which can occupy the $h_{11/2}$ and $i_{13/2}$ single fermion orbits. The calculated energy levels are all in satisfactory agreement with the observed values for these three isotopes. The effect of the introduction of the fermion-pair degrees of freedom was manifested in the improvement of the calculated energy levels when we compare with the previous results obtained by a pure IBA calculation.[19]

[1]C. Schück, M. A. Deleplanque, R. M. Diamond, F. S. Stephens, and J. Dudek, Nucl. Phys. **A496**, 385 (1989).

[2]F. S. Stephens, M. A. Deleplanque, R. M. Diamond, A. O. Macchiavelli, and J. E. Draper, Phys. Rev. Lett. **54**, 2584 (1985).

[3]J. Simpson, M. A. Riley, J. R. Cresswell, P. D. Forsyth, D. Howe, M. B. Nyako, J. F. Sharpey-Schafer, J. Bacelar, J. D. Garrett, G. B. Hagemann, B. Herskind, and A. Holm, Phys. Rev. Lett. **53**, 648 (1984).

[4]M. Oshima, N. R. Johnson, F. K. Mcgowan, C. Baktash, I. Y. Lee, Y. Schutz, V. Ribas, and J. C. Wells, Phys. Rev. C **33**, 1988 (1986).

[5]P. O. Tjøm, R. M. Diamond, J. C. Bacelar, E. M. Beck, M. A. Deleplanque, J. E. Draper, and F. S. Stephens, Phys. Rev. Lett. **55**, 2405 (1985).

[6]M. A. Riley, J. D. Garrett, J. F. Sharpey-Schafer, and J. Simpson, Phys. Lett. B **177**, 15 (1986).

[7]E. M. Beck, H. Hübel, R. M. Diamond, J. C. Bacelar, M. A. Deleplanque, K. H. Maier, R. J. McDonald, F. S. Stephens, and P. O. Tjøm, Phys. Lett. B **215**, 624 (1988).

[8]O. C. Kisner, A. W. Sunyar, and E. der Mateosian, Phys. Rev. C **17**, 1417 (1978).

[9]S. W. Yates, I. Y. Lee, N. R. Johnson, E. Eichler, L. L. Riedinger, M. W. Guidry, A. C. Kahler, D. Cline, R. S. Simon, P. A. Butler, P. Colombani, F. S. Stephens, R. M. Diamond, R. M. Ronningen, R. D. Hichwa, J. H. Hamilton, and E. L. Robinson, Phys. Rev. C **21**, 2366 (1980).

[10]R. Janssens, Y. El Masri, J. M. Ferte, C. Michel, J. Steyaert, and J. Vervier, Nucl. Phys. **A283**, 493 (1977).

[11]R. G. Helmer, Nucl. Data Sheets **52**, 1 (1987).

[12]R. G. Helmer, Nucl. Data Sheets **49**, 383 (1986).
[13]M. A. Lee, Nucl. Data Sheets **56**, 199 (1989).
[14]E. N. Shurshikov, Nucl. Data Sheets **47**, 433 (1986).
[15]F. S. Stephens and R. S. Simon, Nucl. Phys. **A183**, 257 (1972).
[16]A. Arima and F. Iachello, Phys. Rev. Lett. **35**, 1069 (1975); **40**, 385 (1978); Ann. Phys. (N.Y.) **99**, 253 (1976); **111**, 201 (1978); **121**, 468 (1979).
[17]D. S. Chuu and S. T. Hsieh, Phys. Rev. C **38**, 960 (1988), and references therein.
[18]D. R. Zolonowski, M. B. Hughes, J. Hunt, and T. T. Sugihara, Phys. Rev. C **21**, 2556 (1980).
[19]C. S. Han, D. S. Chuu, S. T. Hsieh, and H. C. Chiang, Phys. Lett. **163B**, 259 (1985).
[20]N. Yoshida and A. Arima, Phys. Lett. **164B**, 231 (1985).
[21]H. Harter, A. Gelberg, and P. Von Brentano, Phys. Lett. **157B**, 1 (1988).
[22]D. S. Chuu, C. S. Han, S. T. Hsieh, and M. M. K. Yen, Phys. Rev. C **27**, 380 (1983).
[23]S. T. Hsieh, M. C. Wang, and D. S. Chuu, Phys. Rev. C **23**, 521 (1981).
[24]H. Emling, E. Grosse, R. Kulessa, D. Schwalm, and H. Wollersheim, Nucl. Phys. **A419**, 187 (1984).